Joint EPRI – 123HiMAT International Conference on
Advances in High Temperature Materials
October 21–24, 2019, Nagasaki, Japan
J. Shingledecker, M. Takeyama, editors
https://doi.org/10.31339/asm.cp.am-epri-2019p1123

CREEP AND FAILURE BEHAVIOR OF WELDED JOINTS MADE OF ALLOY 617B

Annett Udoh, Magdalena Speicher, Andreas Klenk
Material Testing Institute University of Stuttgart, Stuttgart, Germany

ABSTRACT

Welded joints of Ni-base alloys are often the critical part of components operated under high temperature service conditions. Especially welds in thick-walled structures are susceptible to various crack phenomena. Creep rupture and deformation behavior of different similar welds of Alloy 617B, both circumferential and longitudinal, were determined in many research German projects with the aim to qualify the nickel alloys and its welded joints for the use in highly efficient Advanced Ultra Supercritical (AUSC) power plants. Damage mechanisms and failure behavior have also been investigated within these projects. In order to reduce the welding residual stresses in thick-walled components a post weld heat treatment (PWHT) for Alloy 617B is recommended after welding. This PHWT reduces not only residual stresses but causes changes in the damage mechanisms and failure behavior of welded joints of Alloy 617B. Improving effects of PWHT have been investigated in this study and results of microstructural investigations were correlated with the material behavior.

INTRODUCTION

As long as coal-fired power plants play an important role in securing the energy supply, minimizing CO_2 emissions when operating them is of great importance. With use of new technologies in steam power plants, which are based primarily on the significant increase in the steam parameters (pressure and temperature), an increase in efficiency and a reduction in pollutant emissions can be achieved. Conventional materials are not suitable for this high temperature and stress range, therefore nickel-base alloys must increasingly be used. In particular, the properties of components with larger wall thicknesses, which represent a new field of application for these materials and the properties after the application of necessary manufacturing steps such as induction bending and welding have to be characterized. In particular, the increase in temperature places considerable demands on the proof of the long-term stability with regard to corrosion (oxidation), microstructure, strength and deformability of the used materials. Without that, safe operation without endangering man and the environment is not possible. The aim of the investigations within different research projects [1-7] was to create a reliable database with characteristic values for the specific, long-term changing of material properties of nickel-base alloys and their weld joints, which in principle should be suitable for meeting the criteria of the Pressure Equipment Directive.

MANUFACTURING OF WELDED JOINTS MADE OF NICKEL ALLOYS

More than 20 years ago, the first projects in Germany were initiated [1, 2] with the goal of qualifying the materials for new high efficient coal-fired power plants. The focus was on the qualification and adaptation of welding processes, especially for thick-walled structures. For example the investigations in [1] showed that an optimization of the welding consumables for welded joints made of Alloy 617 aimed to avoid melting losses was successfully applied. Cross weld creep tests indicated that weld performance could be improved, however tests must be continued in order to get a reliable long-term data base for weldments. The results of the welding procedure qualifications (WPQ) and the welding which was done to manufacture components shown the applicability of the welding processes described there. Problems like hot cracking could be avoided and the requirements given in codes and standards could be fulfilled. First experiences from field tests were obtained in [4, 5] and showed the possibilities of applying this material to USC plants.

A special challenge and interesting issue was the manufacturing of longitudinally welded pipe performed in [7]. There, a welding procedure for the production of such seam welds was developed and the welded joints produced with optimized parameters has been examined a comprehensive qualification test program.
The aim of the optimizing the welding process was to achieve a high deposition rate and to minimize the burn up of alloying elements such as Al, Ti, Cr, etc. For that systematic investigations were carried out in which the welding parameters were varied and each weld joint was examined by metallographic methods. Cracks along the grain boundaries in the heat affected zone should be avoided. The weld joint geometry and the opening angle were optimized as well as the arc characteristics of the metal inert gas welding process (intert gas, contact tube distance, wire feed speed, arc voltage and current intensity). The weld beads had notch-free transitions. Furthermore, the influence of the interpass temperature was checked, the plating of the seam flank and the conversion of tensile to compressive stresses by hammering of the seam. When preparing the weld, it has to be taken into account that the properties of nickel-base alloys can change during solidification through mechanical processing. The machining parameters (cutting depth and cutting speed) must be adapted to the material.
A narrow gap counter-milling (radius = 3 mm, opening angle = 8 °) was performed before welding. Following the milling, the flank area was tested for discontinuity over the entire length using indentation. The findings were in accordance with the specifications without any notifiable signals. After a tungsten inert gas (TIG) root welding, the external welding with the same filler material was also carried out fully mechanically by TIG welding. The heat input was between 0.8 kJ / mm and 1.1 kJ / mm. The inert gas used was VARIGON H5, a inert gas consisting of 95% argon with 5% helium (DIN EN ISO 14175: R1 - ArH5). The filler used was a S Ni 6617 (NiCr22Co12Mo9). The maximum interpass temperature was 76 °C. After completion of the weld, the pipe was calibrated in an O-press to an ovality of 0.5%. The final dimensions of the welded pipe were 542 mm of outer diameter and 31.5 mm of wall thickness.
In this case, the results of the welding procedure qualifications (WPQ) and the qualification testing also showed the applicability of the welding processes used in [7].

BEHAVIOR OF WELDED JOINTS AT HIGH TEMPERATURES

Different similar welded joints made of Alloy 617B on pipes, tubes, plates and forging pipe with different base materials and weld metals were produced using different welding processes (shielded metal arc, tungsten inert-gas: manual and orbital, submerged arc, electron beam welding). In total 21 seams (20 circumferential seams and 1 longitudinally welded pipe) were investigated and qualified in many research projects [1-7], also in component like test in the lab as well as in the test loop in a Grosskraftwerk (GKM) in Mannheim in Germany [4, 5].

The nominal chemical composition and the parameter of the heat treatment for Alloy 617B are summarized in Table 1.
All materials were welded in the solution annealed condition and inspected by non destructive testing (NDT). To characterize the deformation and failure behavior creep, rupture tests were carried out within the temperature range of 600 to 750 °C on welded joints (cross weld specimens), selected weld metals and base material. The cross weld specimens were examined in the as-welded condition, as well as after the post weld heat treatment at 980 °C for 3 hours followed by cooling in air. Additionally the measurement of residual stresses on the components (pipes) was performed. The microstructure of selected welded joints was characterized using optical microscopy (OM) and transmission electron microscopy (TEM) after creep testing. For the TEM analysis, metal foils were prepared by spark erosion, mechanical cutting, grinding and chemical etching using a Tenupol-3 from Struers. TEM investigations were performed using a JEOL JEM 2010F operated at 200 kV to determine the precipitation state and the dislocation density. For analytical measurements using energy dispersive X-ray spectroscopy (EDX) the TEM is equipped with an EDX detector (Apollo XLT2 from EDAX). EDX mappings have been recorded at several locations at grain boundaries and within the grains. The quantitative measurement of the particles has been done with the software ImageJ.

Table 1: Chemical composition and parameters of the heat treatment according to [8]

	Chemical composition (wt.%)							
Material	C	Cr	Mo	Co	Al	Ti	Fe	B
Alloy 617B	0.05-0.008	21.0-23.0	8.0-10.0	11.0-13.0	0.8-1.3	0.25-0.5	1.5	0.001-0.005
	Parameters of heat treatment							
	1150 - 1200 °C / up to 5 h (forging parts) / Water							

Residual stress

The influence of the PWHT at 980 °C for 3 h on the level of the residual stresses in welded pipes made of Alloy 617B was investigated for selected components. Residual stress measurements were carried out by the borehole method before and after 980 °C annealing in the area of weld metal and heat affected zone, Figure 1.

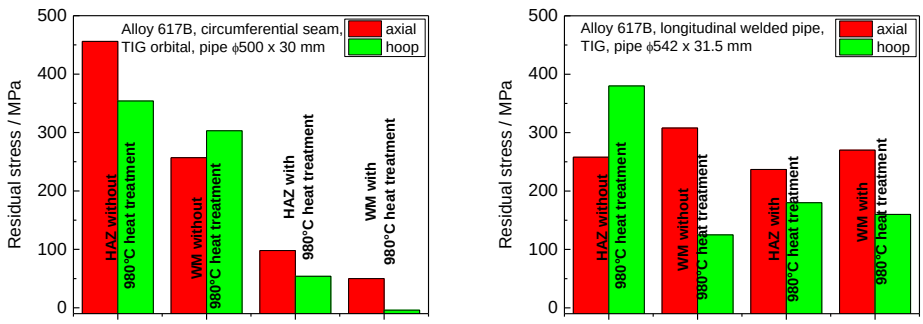

a) b)

Figure 1: Results of residual stress measurement of a) pipe with circumferential seam (TIG orbital) and b) longitudinal welded pipe (TIG) before and after annealing at 980 °C for 3 h

The residual stresses before annealing at 980 °C are high, especially in the area of the heat affected zone / the fusion line. The values of the residual stresses are near to the yield strength of the material. Due to the annealing, the residual stresses can significantly be reduced. This could also be confirmed by the measurement with the ring core method, which allows statements about a greater depth compared to the drill hole method.

Creep behavior

The results of creep rupture tests of welded joints at 700 °C and 750 °C are shown in Figure 2. For the comparison the scatter band from [8] for base material is also shown here.
In the short-creep regime (700 °C) an influence of the PWHT at 980 °C for 3h can be seen. If the specimens were heat treated, the fracture position is shifted from the weld metal into the base material. Thus, the creep rupture strength of the cross weld specimens increased. If the location of fracture doesn't change after PWHT, the creep rupture time increases at the same level of stress. The similar effect can also be observed in the long-term region. After applying PWHT the failure behavior changes and the fracture is mostly located in the base material. All heat-treated cross weld specimens reach the upper scatter band for the base material in the investigated temperature range. In addition, improved creep rupture strength of the produced welds has been achieved over the years due to optimized and further improved manufacturing and processing technologies as well as the optimized consumables.

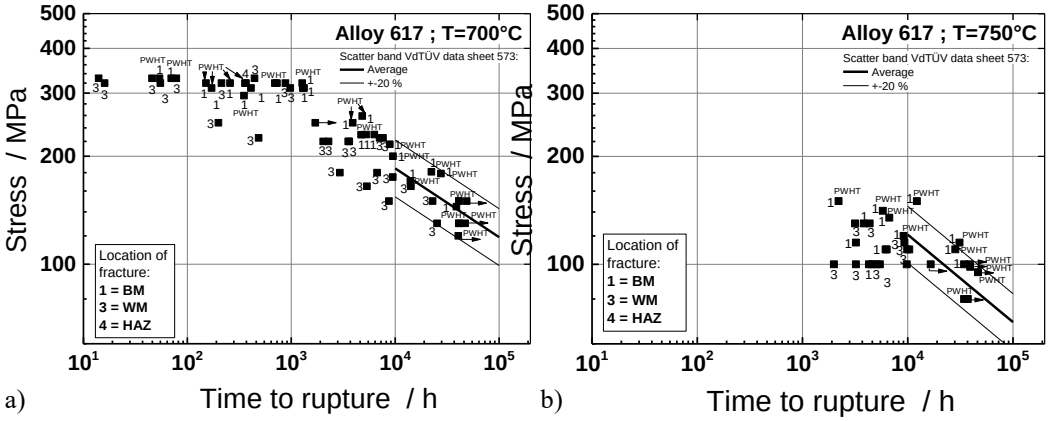

Figure 2: Creep rupture behavior of Alloy 617B and its welded joints a) at 700 °C and b) at 750 °C (PWHT=after applying 980 °C for 3 h)

DAMAGE EVOLUTION

Using optical microscopy damage evolution was investigated in different cross weld specimens after creep rupture tests. Figure 3 shows microstructure in different areas of a welded joint in as-welded condition and after creep loading. The microstructure in the initial state consists of an austenitic matrix with randomly distributed carbides and carbonitrides of type Ti (C, N). The grain structure in the base material is inhomogeneous. The microstructure in the weld metal is dendritic. In the as-welded condition no welding defects such as hot cracks or lack of fusion were observed in the welded joint. After creep loading in a short-time region numerous separations of grain boundaries without cavity formation could be seen. The microcracks occur, often as wedge cracks at the grain triple points, which suggests the grain boundary sliding as the creep mechanism, typically at high loads. All cracks are concentrated along the grain boundaries. The crack paths are,

depending on fracture location, interdendritic in the weld metal and intergranular in the base material. The heat affected zone (HAZ) area was free of cracks.
After long-term creep test (for about 27,000 h), interdendritic cracks also appeared in the weld metal without formation of creep cavities in the specimen tested in as-weld condition, see Figure 2 e. The creep cavities could be observed in the base material near the fusion line (Figure 2 f). The cavities at grain boundaries are situated perpendicular to the loading direction.

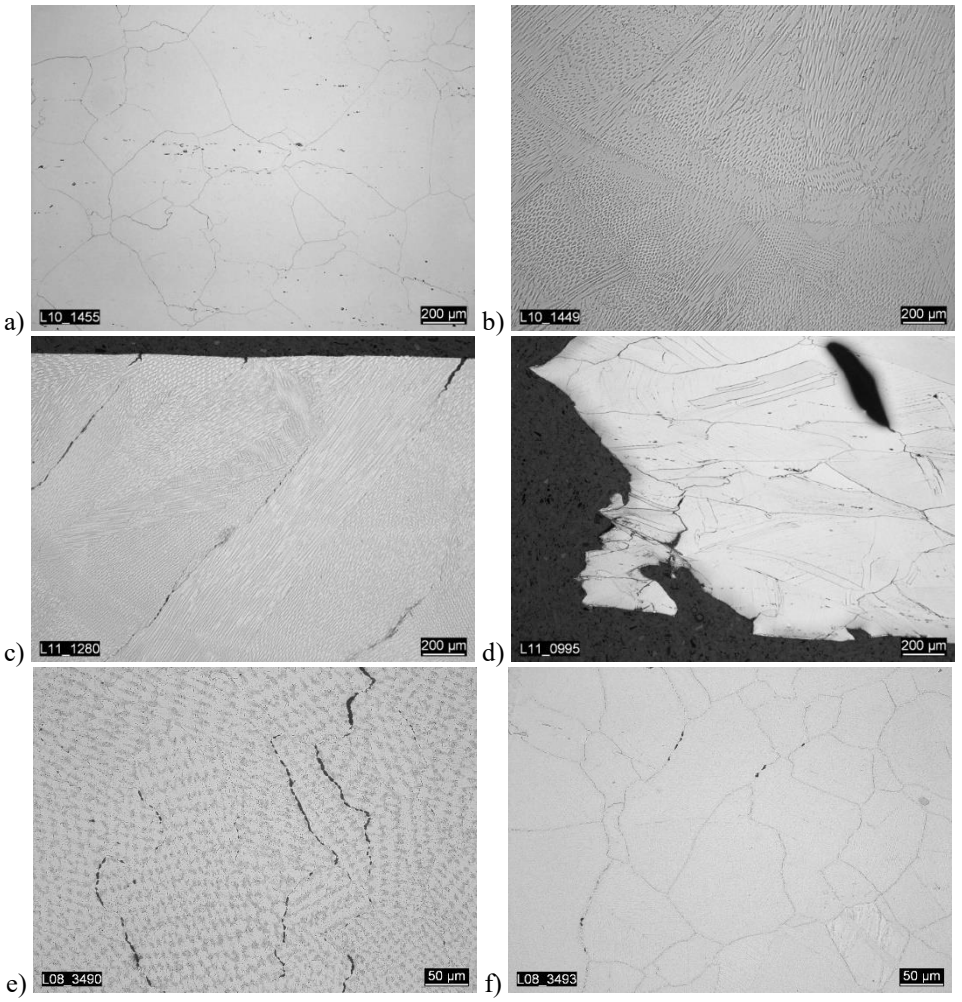

Figure 3: Optical images of initial states a) base material, b) weld metal; after short-term creep test c) fracture in weld metal (without PWHT), d) fracture in base material (with PWHT), after long-term creep test e) fracture in weld metal (without PWHT), f) damage in base material (without PWHT)

MICROSTRUCTURE INVESTIGATIONS

The effect of the applying the PWHT on the creep rupture behavior of welded joints was investigated in detail using TEM. This is especially relevant in the short-term creep regime, due to the high probability of failure in the first phase of the service. For this purpose, the specimens after short-term creep loading at 700 °C of welded joints of Alloy 617B in as-welded condition, after

PWHT at 980 °C and after creep loading was investigated in the area of base material (BM) and weld metal (WM) [9].
In the as-welded condition, only few $M_{23}C_6$ carbides are found both in the BM and in the WM within the grain and isolated at the grain boundaries. The dislocation density in the weld metal is 10 times higher than in the base material. γ' phase was not identified in any state. After creep at 700 °C, the density of $M_{23}C_6$ carbides within the grain increases. At the grain boundaries the number of particles increase in BM but decrease in WM. γ' phase occurs within the grain in both states. Compared with the non-heat treated initial state more $M_{23}C_6$ carbides are found in both areas (BM and WM) within the grain and at the grain boundaries.
After short-term creep loading there is still a difference between two conditions. In post weld heat treated state, the size of $M_{23}C_6$ carbides within the grain increases, the γ' phase is, however, smaller (Figure 4 a and b). This could be observed for both the base metal and the weld metal. The changes during the creep loading are not significant especially concerning $M_{23}C_6$ carbides in the PWHT state. The density of $M_{23}C_6$ particles in heat treated state does not increase, however it is increasing in the non-heat treated condition, since only few particles were present there before the creep test. The density of γ' phase increases in heat treated condition more than in the initial state.

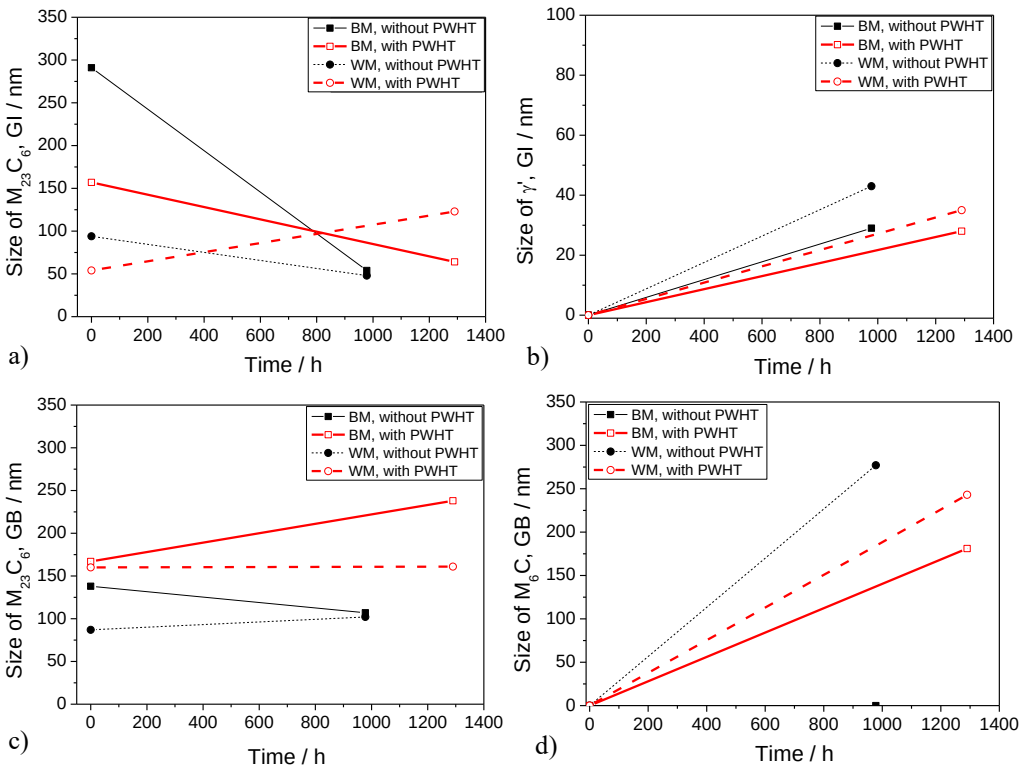

Figure 4: Changes of the precipitates size of a) $M_{23}C_6$ carbides within the grain (GI); b) γ' phase within the grain (GI); c) $M_{23}C_6$ carbides at grain boundaries (GB), d) M_6C carbides at grain boundaries (GB)

From these observations it can be concluded that the PWHT at 980 °C effected a thermal stabilization of the $M_{23}C_6$ within the grain, and causes simultaneously an increased formation of γ' phase due to the reduced precipitation behaviour of $M_{23}C_6$.
At the grain boundaries, the $M_{23}C_6$ carbides are larger by a factor of 2 than within the grain (Figure 4 c). Although the carbides after PWHT are already twice as large as in the untreated state,

they grow continuously, while they rather decrease in the initial state (solution annealed for BM and as-welded for WM). The number of $M_{23}C_6$ carbides increases in both states rather by comparable size. During the creep M_6C carbides are forming (Figure 4 d).
After long-term creep loading (for about 27,000 h at 700 °C) the size of the $M_{23}C_6$ carbides within the grain remains relatively constant at values in the range 30 to 50 nm in a sample which has not been subjected to annealing at 980 °C, see Figure 5. On the other hand, sizes higher than 200 nm (in the heat treated state after 1,400 h approximately 200 nm) are achieved at the grain boundary. In the weld metal, no $M_{23}C_6$ carbides can be found any more, but M_6C precipitates (151 nm) are observed within the grain, which are significantly larger at the grain boundaries (265 nm). The size of the γ' phase within the grain increases further to values of 90 nm (after approximately 1,000 h - 20 to 40 nm) in the base material or 112 nm in the weld metal.

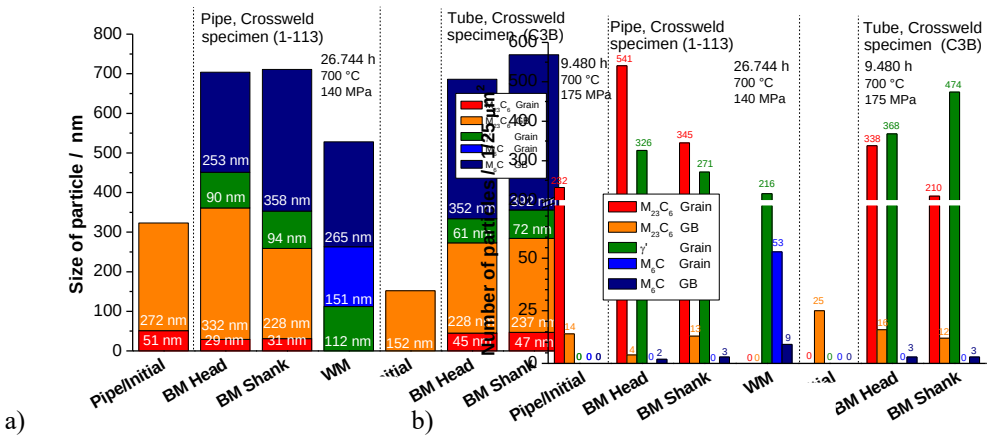

Figure 5: Results of TEM-investigations of a cross weld specimen made of Alloy 617B (pipe) [2] in initial condition and after creep at 700 °C; a) size and b) number of precipitates

Thus, it can be stated that the precipitation structure changes significantly due to creep loading:
The amount of carbides $M_{23}C_6$ within the grain, which form in the base material, increase, their size remains largely unchanged. When the initial state was annealed at 980 °C for 3 h, coarse carbides $M_{23}C_6$ were precipitated. That leads to reduction of the grain strength or decrease grain hardening due to the reduced precipitation of fine $M_{23}C_6$ during creep at 700 °C.
In the investigated weld metal carbides $M_{23}C_6$ does not precipitate within the grain unless 980 °C annealing was performed before creep loading. Rather Mo-rich carbides M_6C were formed. The size of these particles was significantly larger within the grain compared to the $M_{23}C_6$ in the base material (112 nm WM – 31 nm BM). Also at the grain boundary, the particles of M_6C were larger than the particles of $M_{23}C_6$ at the grain boundary in base material (228 nm BM - 265 nm WM).
The amount as well as the size of the γ' phase increases continuously during creep. The number of particles is influenced by the annealing at 980 °C: after annealing a higher density of particles could be observed compared to the not annealed state, which can probably be related to the formation of the $M_{23}C_6$ at the same time.
The differences in the changes of the microstructure within the grain and at the grain boundaries affect the strength and failure behavior of the material. The increasing precipitation of γ' phase in combination with the formation of fine $M_{23}C_6$ promote the strength of the grain, while the coarsening of the particles decreases the strength at the grain boundary.
For time-dependent loading the failure position increasingly shifted towards the grain boundary, which results in a reduction of creep ductility. A PWHT at 980 °C of the initial state causes precipitation of $M_{23}C_6$. Since these are relatively thermally stable and only few new fine $M_{23}C_6$ form due to the already formed precipitates, the grain can absorb more deformation in this state. In

addition, coarsening of the particles at the grain boundaries is lower, so that the grain boundary strength increases compared to the non-heat treated state. Thus, the ductility increases for this material condition and consequently (residual) stress can be better reduced by plastic deformation. If areas of the base material and the weld metal in both states are compared, only low amount of precipitates at the grain boundaries in areas that have failed could be observed (WM without PWHT and BM after PWHT). Thus, there are not enough obstacles that can limit the grain boundary sliding. Due to the high number of intragranural precipitates, the grains are stronger and make strain relaxation along the grain boundaries more difficult, favoring crack formation.

SUMMARY AND CONCLUSIONS

In several research projects in Germany in the past decade, knowledge about the deformation, the failure and the precipitation behavior of similar welded joints of Alloy 617B was obtained. The welding parameters of the examined components were found to be optimal with regard to the production of the seams free from defects. Due to the temperature exposure at 700 °C the microstructure of the material changes and is unstable in the investigated temperature and time range as a consequence of the formation of carbides and γ' phase. Therefore the hardness increase and limited deformability must be expected in welded joints during high temperature application. A post weld heat treatment applied at 980 °C for 3 h after welding leads to a reduction of residual stresses, causes the stabilization of the microstructure and an increase of the deformation capability in all areas of the welded joints.

With regard to the failure behavior, the cross weld specimens of all seams from thick-walled pipes tested in the as-welded condition fail in the creep region in the weld metal. After PWHT a change of fracture position occurs in almost all welds. If the fracture occurred in the weld metal without PWHT, the failure position after PWHT moved into the base material. The crack paths each time concentrate along the grain boundaries (interdendritic in weld metal or intergranular in base material).

Interaction of all these factors mentioned before can determine the failure behavior of the welded joints. Regarding thick-walled welded components made of Alloy 617B the reduction of residual stresses is very important as well as the stabilization of the microstructure, since the two factors are decisive for the failure behavior of the welds and the crack formation.

REFERENCES

[1] Husemann, R. U., A. Helmrich, J. Heinemann, A. Klenk, K. Maile, “Applicabiliy of Ni-based welding consumables for boiler tubes and piping in the temperature range up to 720 °C”, Proc 4th Int. Conf. On Advances in Materials Technology for Fossil Power Plants, October 2004, Hilton Head Island, pp.788-802.

[2] Schmidt, K., Klenk. A., Roos, E., “Qualifying Materials for the 700 /720°-Power Plant-Results from MARCKO700, Part 1: Materials, VGB PowerTech Journal”, Vol. 1-2 (2012), pp.74-84.

[3] Speicher, M. *et al*: COORETEC DE4: Untersuchungen zum langzeitigen Festigkeitsverhalten von Rohren und Schmiedeteilen aus Nickelbasis-Legierungen, Final report BMWi 0327705Y, 2013.

[4] Project 725 HWT GKM Fortsetzung: Untersuchungen zum langzeitigen Betriebsverhalten von Rohren, Guss- und Schmiedeteilen aus Legierungen für zukünftige hocheffiziente Kraftwerke – Fortsetzung (HWT1F), Final report, 2016.

[5] Speicher, M., D. Hüggenberg, A. Klenk, S. Zickler, K. Metzger, “Materials for Advanced Ultra-Supercritical Fossil-Fuel Power Plants: Materials Properties, Microstructure, and Component Behavior”, Energy Technology 4 (2016), pp. 187-192.

[6] Speicher, M., A. Klenk, K. Maile, „Optimierung der Schweißverfahren an Nickelbasislegierungen in dick- und dünnwandigen Kesselbauteilen zur Vermeidung von Fehlern

in hochtemperaturbeanspruchten Schweißnähten“, Final report of research initiative KW21, Part 1, (2013), pp. 366-382.
[7] Udoh, A. A. Klenk, M. Bockelmann, J. Heinemann, „Untersuchungen zum langzeitigen Festigkeits- und Verformungsverhalten von längsnahtgeschweißten Rohren aus der Nickelbasislegierung Alloy 617B“, 46. Sondertagung „Schweißen im Anlagen- und Behälterbau“, München, Februar 2018.
[8] VdTÜV Material data sheet no. 573, Hochwarmfeste Nickelbasislegierung NiCr23Co12Mo; Werkstoff-Nr. 2.4673, 09.2013.
[9] Speicher, M., R. Scheck, K. Maile, „Microstructure-properties correlations in similar welds of Alloy 617“, Sonderbände der Praktischen Metallographie 46 (2014), pp.241-246.